Fault diagnosis of angle grinders and electric impact drills using acoustic signals

Adam Glowacz [1,*], Ryszard Tadeusiewicz [2], Stanislaw Legutko [3], Wahyu Caesarendra [4], Muhammad Irfan [5], Hui Liu [6], Frantisek Brumercik [7], Miroslav Gutten [8], Maciej Sulowicz [9], Jose Alfonso Antonino Daviu [10], Thompson Sarkodie-Gyan [11], Pawel Fracz [12], Anil Kumar [13], Jiawei Xiang [14]

[1] AGH University of Science and Technology, Faculty of Electrical Engineering, Automatics, Computer Science and Biomedical Engineering, Department of Automatic Control and Robotics, al. A. Mickiewicza 30, 30-059 Kraków, Poland; adglow@agh.edu.pl;
[2] AGH University of Science and Technology, Faculty of Electrical Engineering, Automatics, Computer Science and Biomedical Engineering, Department of Biocybernetics and Biomedical Engineering, al. A. Mickiewicza 30, 30-059 Kraków, Poland; rtad@agh.edu.pl;
[3] Poznan University of Technology, Faculty of Mechanical Engineering and Management, 3 Piotrowo Street, 60-965 Poznan, Poland; stanislaw.legutko@put.poznan.pl;
[4] Universiti Brunei Darussalam, Faculty of Integrated Technologies, Jalan Tungku Link, Gadong BE1410, Brunei Darussalam; wahyu.caesarendra@ubd.edu.bn;
[5] Electrical Engineering Department, College of Engineering, Najran University Saudi Arabia, Najran 61441, Saudi Arabia; miditta@nu.edu.sa
[6] College of Quality and Safety Engineering, China Jiliang University, Hangzhou 310018, China; hui.liu@cjlu.edu.cn
[7] Department of Design and Machine Elements, Faculty of Mechanical Engineering, University of Zilina, Univerzitna 1, 010 26 Zilina, Slovakia; frantisek.brumercik@fstroj.uniza.sk;
[8] Department of Measurement and Application Electrical Faculty of Electrical Engineering, University of Zilina, Univerzitna 1, 010 26 Zilina, Slovakia; miroslav.gutten@feit.uniza.sk;
[9] Faculty of Electrical and Computer Engineering, Cracow University of Technology, Warszawska 24 Street, 31-155 Cracow, Poland; msulowicz@pk.edu.pl
[10] Department Electrical Engineering, Universitat Politecnica de Valencia, Instituto Tecnologico de la Energía Camino de Vera s/n, 46022 Valencia, Spain; joanda@die.upv.es
[11] Laboratory for Industrial Metrology and Automation, College of Engineering, University of Texas, El Paso, TX 79968, USA, tsarkodi@utep.edu
[12] Department of Manufacturing Engineering and Automation Products, Opole University of Technology, 45758 Opole, Poland; p.fracz@gmail.com
[13] Amity University Uttar Pradesh, Noida, 201 313, India; anil_taneja86@yahoo.com
[14] College of Mechanical and Electrical Engineering, Wenzhou University, Wenzhou, 325 035, China.; jwxiang@wzu.edu.cn

* Correspondence: adglow@agh.edu.pl

Abstract: Electric motors use about 68% of total generated electricity. Fault diagnosis of electrical motors is an important task, because it allows saving a large amount of money and time. An analysis of acoustic signals is a promising tool to improve the accuracy of fault diagnosis. It is essential to analyze acoustic signals to assess the state of the motor. In this paper, three electric impact drills (EID) were analyzed using acoustic signals: healthy EID, EID with damaged rear bearing, EID with damaged front bearing. Three angle grinders (AG) were analyzed: healthy AG, AG with 1 blocked air inlet, AG with 2 blocked air inlets. The authors proposed a method for feature extraction: SMOFS-NFC (Shortened Method of Frequencies Selection Nearest Frequency Components). Acoustic features vectors were classified by the nearest neighbor classifier and Naive Bayes classifier. The classification accuracy were in the range of 89.33−97.33% for three electric impact drills. The classification accuracy were in the range of 90.66−100% for three angle grinders. The presented method is very useful for diagnosis of bearings, ventilation faults and other mechanical faults of power tools. It can be also useful for diagnosis of similar power tools.

Keywords: degradation, acoustic, fault diagnosis, bearings, power tool, ventilation

1. Introduction

Electric motors and power tools are often used in the industry. Reduction of maintenance costs and proper operation of motors are main goals of fault diagnosis. Financial income can be reduced in the event of production downtimes. Faulty bearings, gears and other mechanical and electrical faults can yield motor shutdowns and hence, interrupt the whole production line. In the industry, many electric motors operate 24 hours per day. This makes a continuous online fault diagnosis necessary. It can be achieved by using computers and proper sensors.

Power tools are used in the industry. Application of power tools can be found in: construction of buildings, industry, home applications, grinding, cutting and drilling. For the mentioned reasons, the authors are motivated to develop new fault diagnostic methods based on acoustic signals. Motivation is also found in the following literature [1−27]. However, most of these works are referred to industrial motors and few works have been devoted to analysis of power tools. In comparison with other techniques, the analysis of acoustic signals is a promising non-invasive tool to improve the accuracy of fault diagnosis of power tools. Moreover, it is an inexpensive technique. It is very attractive for many applications.

To apply the acoustic analysis, it is essential to extract acoustic signal to assess the state of the power tool. The acoustic analysis can be used for diagnosis of different types of motors and faults. In this research 3 EID (electric impact drills) and 3 AG (angle grinders) were analyzed. Each of the analyzed power tool has one state (6 analyzed power tools in total).

The authors proposed a method of feature extraction − SMOFS-NFC (SMOFS Nearest Frequency Components). The article consists of: 1) Introduction, 2) Considered faults of power tools, 3) Theoretical background, 4) proposed approach and experimental setup, 5) Results of acoustic fault diagnosis, 6) Discussion, 7) Conclusions and future work.

2. Considered faults of power tools

Faults of the power tools can be different. There are different mechanical and electrical faults. Mechanical faults, namely: damaged bearings, damaged shaft, broken rotor blades, broken gears, broken teeth, shifted brushes, uneven air gap, misalignment, ventilation faults. On the other hand, some examples of electrical faults of power tools are: broken rotor coils, shorted stator coils, shorted rotor coils, degraded rotor/stator coil insulation. Approximate failure rates of electric motors are as follows: bearings faults ~ 40%, rotor faults ~ 10%, insulation faults ~40%, others types of faults – 10% [1].

Ball bearings are used by the motor of power tools. Normal operation of the motor causes abrasion of bearing parts. Operation of faulty bearing usually yields increases in the sound level. Moreover, acoustic signals of different state of the EID/AG have different frequency spectra.

Acoustic signals of Verto 50G515 electric impact drills (500 W) were measured. The acoustic signals were measured and analyzed for the following cases: healthy EID (Fig. 1), EID with damaged rear bearing (Fig. 2), EID with damaged front bearing (Fig. 3). Rear bearing has a diameter of 0.2 m. Front bearing has a diameter of 0.3 m.

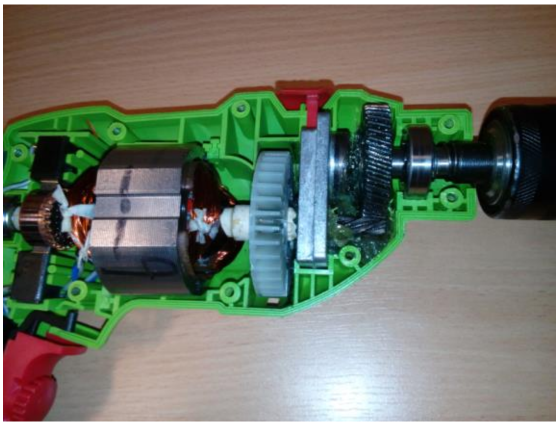

Figure 1. Healthy EID

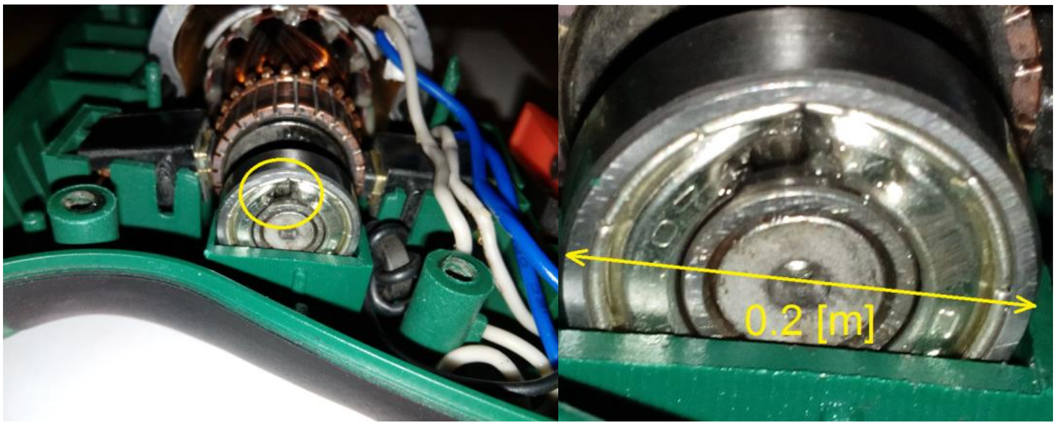

Figure 2. EID with damaged rear bearing (indicated by yellow circle)

Figure 3 EID with damaged front bearing (indicated by yellow circle)

Acoustic signals of Verto 51G053 angle grinders (500W) were also measured. The acoustic signals were measured and analyzed for the following cases: healthy angle grinder (Fig. 4), angle grinder with 2 blocked air inlets (Fig. 5), angle grinder with 1 blocked air inlet (Fig. 6).

Figure 4. Healthy angle grinder

Figure 5. Angle grinder with 2 blocked air inlets

Figure 6. Angle grinder with 1 blocked air inlet

3. Theoretical background

Various types of diagnostic signals are used by fault diagnosis systems. Vibrations, acoustic signals, thermal signals and current signals are often used for fault diagnosis. Each of them has advantages and disadvantages. Fault diagnosis based on electrical signals were described in following papers [2–7]. They require the connection of an ammeter/sensor to measure the electrical signal. Wireless sensors can be also used. The analysis of electrical signals is an interesting research topic. However, it is often limited to electrical faults such as: rotor and stator faults. Moreover, it can be only used in electric motors; it is not good for mechanical engines. It can localize the fault.

Paper [2] presented a method to integrate vibration analysis and current analysis. Wavelet packet decomposition and support vector machines were used for the analysis [2]. Reference [3] described a novel approach for gear fault diagnosis of the three-phase motor using Park and Concordia transforms and Frenet-Serret equations. The obtained results were good for healthy and faulty conditions [3]. Inter-turn winding faults were analyzed in [4]. The authors of the paper analyzed two methods: Zero-sequence voltage component (ZSVC) and motor current signature analysis (MCSA). The ZSVC was more sensitive than the MCSA for inter-turn faults [4]. Reference [5] presented an approach using MCSA, Independent component analysis (ICA) and neural network for detection of broken bar of induction motors. The authors of the paper conducted analysis and obtained classification accuracy in the range 90–99% [5]. Reference [6] described mechanical fault detection of squirrel cage induction motors. It was based on the Fast Fourier Transform (FFT) of the stator current signal. The authors of the paper used the discrete wavelet transform. The MCSA-DWT technique was presented [6]. The authors of the paper presented fault diagnosis using stator current of three-phase induction motor [7]. They used frequency spectral subtraction using: wavelet packet decomposition, discrete wavelet transform, stationary wavelet transform [7].

Another well-known technique using vibration data analysis. Vibrations are good diagnostic signals for electric motors and mechanical engines [8–14]. In general terms, electrical and mechanical faults can be measured and analyzed using vibrations. Vibration analysis enables to detect a faulty state of the machine. Localization of the fault can be more difficult using vibration signals. There are also technical difficulties of the proper position of the sensor and noise contamination.

In [8], the authors dealt with fault diagnosis of rolling bearings. The authors of the paper used graph spectrum coefficients in the highest order range. Next, they used the Hilbert envelope spectrum. The proposed method was noise tolerant and effective for rolling bearings [8].

On the other hand, [9] described fault diagnosis of vibration signals using parameterized time-frequency transform (PTFT) and Polynomial chirplet transform (PCT). Bearing faults were detected using maximum correlated kurtosis deconvolution-based envelope order spectrum. The proposed method was efficient for bearing fault diagnosis under varying speed conditions [9]. Fault diagnosis approach based on the multi-scale fuzzy measure entropy (MFME) was presented in [10]. Bearing fault diagnosis was carried out using MFME and support vector machine. The presented results showed that the proposed approach was efficient [10]. Multi-Input Single-Output model was presented for fault diagnosis of gearbox [11]. Vibration data acquired from a gearbox were analyzed. Conducted analysis showed that the proposed approach was good for extracting the meshing frequency component [11]. A fault diagnosis approach using Convolutional Neural Networks and Extreme Learning Machine was proposed in [12]; the authors of the paper used Continuous Wavelet Transform for preprocessing of vibration signal, while a Convolutional Neural Networks extracted features. The proposed method was effective for vibration analysis of gearbox and bearing. The proposed approach can recognize different types of faults [12]. In [13], a convolutional neural network method was used for vibration signals of gear faults. Training and test vibration signals were measured for different faults. The different faults were recognized properly [13]. Vibration signal of rolling bearing using empirical mode decomposition was analyzed in [14]. The authors used crest factor, kurtosis, skewness, for fault diagnosis. The empirical mode decomposition was good for analysis of roller bearings [14].

Thermal analysis has been also used for fault diagnosis [15–18]. Thermal (infrared) images are good diagnostic signals for electrical faults (electrical insulation faults, rotor, stator faults) and for specific mechanical faults (for example bearings faults). However thermal imaging is often expensive. Processing of thermal images is slower than processing of acoustic, vibration or electric current signals. Infrared imaging is based on measuring the superficial temperatures of the object. Thermal imaging camera needs time to measure the change of temperature. Faulty and healthy motors need time to heat up.

In [15], infrared thermal images and a convolutional neural network were used for fault diagnosis of a gearbox. The proposed approach was efficient for gear faults: cracks, breakages, tooth pitting [15]. In [16], thermal phenomena of the kinematic chain of the induction machine was analyzed using an infrared thermography technique; it was based on the analysis of the segmentation of thermal image. The proposed technique is useful for locating the damage and influence of the damage [16]. Reference [17] described thermal signature analysis of the brushed DC motor. The authors of the paper used thermocouples with the data logger. Thermocouples were mounted on different machine parts. Healthy DC motor and commutator fault DC motor were recognized using characteristic temperature profile of the DC motor [17]. A fault diagnosis method using thermal images of bearings was presented in [18]. The authors of the paper used bag-of-visual-word and convolutional neural network. The described method was used to analyze test images of bearings. The obtained results showed that it was efficient method of fault diagnosis [18]. Reference [19] described feature extraction of thermal images BCAoID. The BCAoID method was used for three electric impact drills. The recognition results of the performed analysis were in the range of 97.91–100%.

Acoustic signal analysis is also interesting diagnostic technique [20–30]. It can be used to detect and localize faults of the machine. A microphone array is a suitable equipment for localization of faults using acoustic analysis. However, one-channel microphone is less expensive. Moreover, the processing of one-channel signal is faster for recognition. Acoustic analysis is proper for mechanical and electrical faults.

In [20], it is shown that the sound and vibration levels of a diesel engine are different for different states of engine [20]. The FFT and statistical feature extraction methods were used in that work for the analysis of the liner scuffing fault. The results showed that the presented methods were adequate for the recognition of this fault. Moreover, the acoustic emission level of the analyzed machine was increased [20]. In [21], fault diagnosis of low-speed bearings was considered; the analysis was carried out using support vector machines and genetic algorithms. Three classes were used for the analysis. The methods of the analysis of acoustic signals were suitable for the detection of bearing faults. On the other hand, in [22] the authors proposed a wayside acoustic defective bearing detector system for bearing fault diagnosis. The obtained simulation and experimental results showed that the presented method using microphone array can be helpful for fault diagnosis [22]. Vibration and acoustic signals were used for fault diagnosis of bearing defects. Both signals were processed. Next signals were classified by the K-nearest neighbor. Vibration signals were useful for detection of inner race and outer race defects. Besides, acoustic signals were helpful for detection of ball defects [23]. Acoustic fault detection of rotating bearings was described in [24]. A single microphone was used for capture sound signal. Kernel linear discriminant analysis, K-nearest neighbor classifier, support vector machine and sparse discriminant analysis were used for processing the acoustic signals. Ball defects as well as inner and outer race faults were recognized properly [24]. An acoustic-based fault detection of the induction motor was presented in [25]. Bearing faults, single phasing, broken rotor bars were analyzed. Rational-dilation wavelet transform was used to extract feature vector. Acoustic signals of faults had better representation of faults using Q-factor filters [25]. In [26], a single stage spur gearbox was diagnosed using acoustic signals. The authors of the paper used continuous wavelet transform. The results of conducted analysis showed that acoustic signals are effective for fault diagnosis of the gearbox [26]. In [27], vibration and acoustic signals were used for gear fault diagnosis; the analysis of signals was based on the general linear chirplet transform. The results proved that non-contact acoustic measurement and the proposed method of fault diagnosis is useful for gear condition monitoring [27]. A review of fault diagnosis of multi-sensors information fusion for rolling bearings was presented in [28]. In [29], the authors collected acoustic signals of roller bearings and deep graph convolutional network was used for processing of acoustic data. Acoustic data were transformed into graphs. Next, the deep graph convolution network used the training sets of graphs. Testing accuracy was in the range of 80-100%. The experimental results showed usefulness of the deep graph convolutional network for fault detection [29]. Finally, in [30], acoustic signals were also used for technical condition estimation of defects of on-load tap-changers. The authors of the paper showed usefulness of acoustic analysis.

Technical diagnosis is very important from economic point of view. For instance, the collaborative alliance of national metrological organizations from member states of the European Union EURAMET in 2014 published the roadmap for thermometry [31], where it declared the problem of creating the sensors with selfvalidation as one of the key problems of metrology. Even new devices appear to fit the recommendations from the roadmap [32, 33]. The problem of diagnosis is not new in many areas [34-36]. However, it is always preferable to carry out noninvasive diagnosis in order not to change the existing devices and sensors. That is why a lot of attention is now paid to develop the noninvasive methods of diagnosis, especially when such procedure is possible during normal operation of devices and appliances.

In summary, there are many methods of fault diagnosis of bearing, namely: vibration, acoustic, oil, temperature and ultrasonic analysis. Each type of signal has its own advantages and disadvantages. Acoustic analysis is low-cost, fast and non-invasive, but it is easy to be interfered by background noise. Vibration analysis has high recognition rate. It can detect several faults of the motor. It is difficult to localize fault. Vibration signal is not noisy. Analysis of thermal images can detect and localize fault, but it is not fast. The motor needs time to heat up. It is also expensive analysis.

4. The proposed approach and experimental setup

Measurements were carried out in a 4.5x4.5 m room. The walls of room consisted of bricks. Acoustic signals were generated by operation, rotations, friction of bearings, shaft, gear and other parts of the power tool. To measure the acoustic signals, the authors used a notebook and a microphone (tracer KTM 43948). The main characteristics of the microphone were: sensitivity 58 dB +/-3 dB, frequency response 30–16,000 Hz. Distance between microphone and the power tool was equal to 0.5 m.

Acoustic signals were acquired and saved as .WAV digital files. The sampling rate of each .WAV file was equal to 44,100 Hz. The number of channels was equal to 1. To compare the .WAV files, the authors used 1-s samples. The length of sample was equal to 1 second (44,100 values). It was enough to recognize signal properly. To compare sound level of each sample, the authors used amplitude normalization in the range of -1 to 1. It was easier to compare samples measured for example from distance 0.5 m and 0.1 m. In order to avoid difficulties, the authors measured all acoustic signals from the same distance. After that, SMOFS-NFC method was applied to compute selected features. Next, the features were used for computation of feature vectors. The next step was the classification. The classification methods were: Nearest Neighbor, Naive Bayes classifier. The Nearest Neighbor was used for the computation of the distances between feature vectors (training vector and test vector). The result of recognition was a name of recognized class for example 'healthy_EID'. A flowchart of the proposed approach was shown in figure 7.

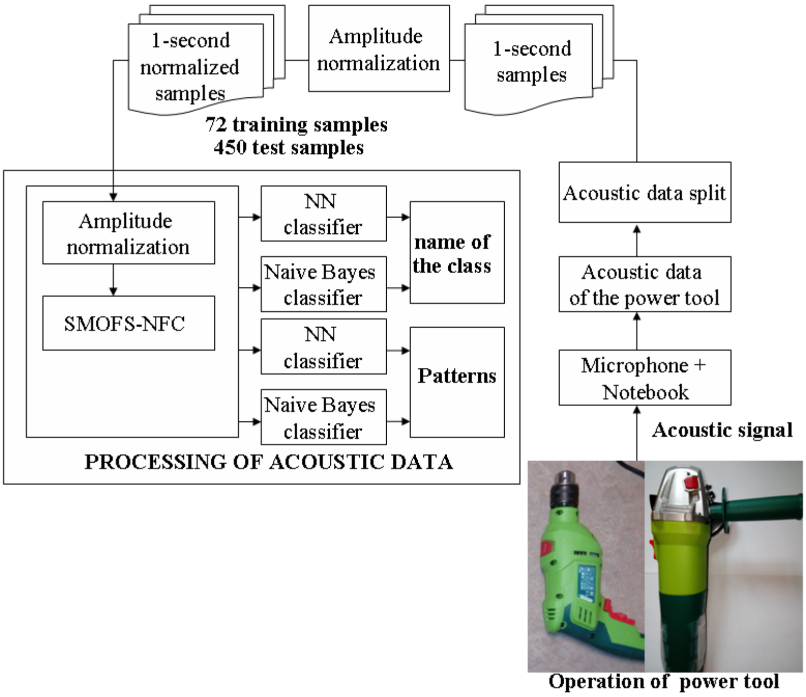

Figure 7. Flowchart of the proposed approach

Proposition of an experimental setup is shown in Figure 8. The experimental setup uses acoustic signal of power tools (electric impact drills and angle grinders), microphone and notebook (personal computer), software of processing acoustic data.

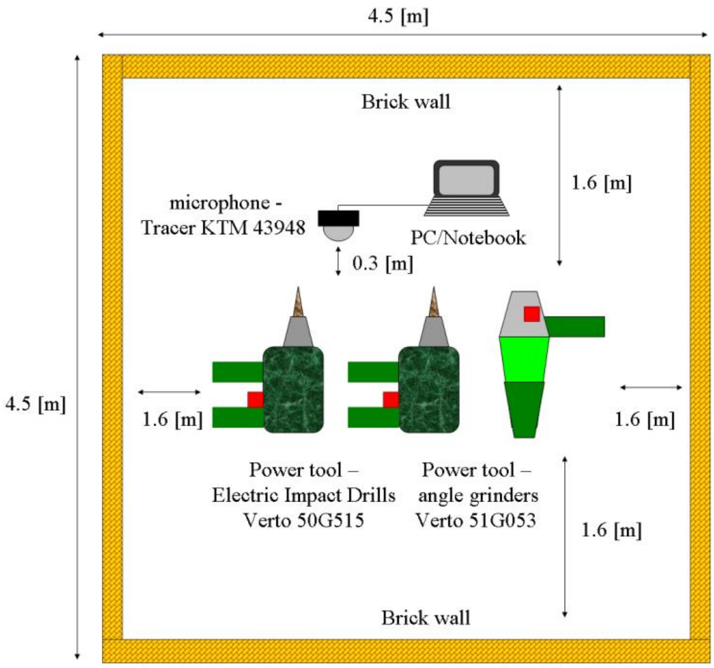

Figure 8. Experimental setup

4.1. SMOFS-NFC (SMOFS Nearest Frequency Components)

The proposed approach of fault diagnosis is based on the SMOFS-NFC method. The SMOFS-NFC is a feature extraction method. It analyzes FFT spectrum of acoustic signal. It computes adjacent frequency components. Next it computes feature vectors. Steps of the SMOFS-NFC are following:

1. Use FFT (Fast Fourier Transform) method to compute frequency spectrum of an acoustic signal. If we have 3 different electric drills, then it requires to compute 3 frequency spectra of acoustic signals. A vector of 16,384-elements is formed. Each element of the vector is a frequency component (1.345825 Hz, 22,050/16,384 ≈ 1.345825). Following 16,384-elements vectors are computed for 3 classes: healthy EID − **h**=[h_1, h_2, ..., h_{16384}], EID with damaged rear bearing − **r**=[r_1, r_2, ..., r_{16384}], EID with damaged front bearing − **f**=[f_1, f_2, ..., f_{16384}].
2. Subtract one frequency spectrum from another: **h - f, h - r, f - r.**
3. Compute: |**h - f**|, |**h - r**|, |**f - r**|.
4. Automatically set a threshold TSM_n of the SMOFS-NFC method. If frequency component is greater that a threshold TSM_n (initially TSM_n = (*sum of all absolute values of frequency components* / 16,384) and TSM_n is increasing), next select frequency component (1).

$$||X_1|-|Y_1||>TSM_n, \tag{1}$$

where TSM_n – threshold of the SMOFS-NFC method for *n-th* iteration, $|X_1|$,$|Y_1|$ – frequency components of different signals with the same index for example $|h_1 - f_1|$ or $|h_{1000} - r_{1000}|$ or $|f_{16384} - r_{16384}|$ and **h**=[X_1, ..., X_{16384}], **f**=[Y_1, ..., Y_{16384}], **r**=[r_1, r_2, ..., r_{16384}].

5. Increase threshold TSM_n. Threshold TSM_n is computed by following equation (2):

$$TSM_n = \frac{\sum_{NF_n=1}^{NF_n} \| X_1 | - | Y_1 \|}{NF_n}, \tag{2}$$

$$NF_n \le 18, \tag{3}$$

where NF_n − Number of frequency components after *n-th* iterations. At the start NF_n is equal to 16,384. This number is decreased for each iteration. If $NF_n \le 18$, then iterations are stopped (3). If $NF_n > 18$, then SMOFS-NFC uses formula (2). The value of TSM_n is increased. The SMOFS-NFC method finds 1-18 frequency components. The values of TSM_n, NF_n, number of iterations n depend on frequency spectra of acoustic signals. The maximum value of NF_n (value of 18) is set experimentally.

For example,

initial threshold_h_f = ((h_1-f_1)+(h_2-f_2)+....+(h_{16384}-f_{16384}))/ 16384 = 0.00048897 (Fig. 13).

initial threshold_h_r = ((h_1-r_1)+(h_2-r_2)+....+(h_{16384}-r_{16384}))/ 16384 = 0.00049407 (Fig. 14).

initial threshold_f_r = ((f_1-r_1)+(f_2-r_2)+....+(f_{16384}-r_{16384}))/ 16384 = 0.00046504 (Fig. 15).

If the value of frequency coefficient is below the threshold, frequency coefficient is removed. If the value of frequency coefficient is above the threshold, then frequency coefficient is used for further computation. The threshold is changeable. Each iteration means new higher threshold and less analyzed frequency components (please see Fig. 13 –

Fig. 15). If the remaining frequency components **x**, **y**, **z** have length ≤18 elements then we do not compute a new threshold, where **x**, **y**, **z**, − vector consisted of remaining frequency components after *n*-th iteration (for example, sixth iteration, 8 frequency components).

final threshold_h_f=($(h_1$-$f_1)$+....+$(h_x$-$f_x)$)/length(**x**)=0.0079 (Fig. 13), after sixth iteration,

final threshold_h_r=($(h_1$-$r_1)$+....+$(h_y$-$r_y)$)/length(**y**)=0.0100 (Fig. 14), after sixth iteration,

final threshold_f_r = ($(f_1$-$r_1)$+....+$(f_z$-$r_z)$)/length(**z**) = 0.0079 (Fig. 15), after sixth iteration, where length(**x**) ≤ 18, length(**y**) ≤ 18, length(**z**) ≤ 18.

The value of final threshold is depended on type of analyzed acoustic signals. We set only the length of final feature vector for example 1−18 elements. The threshold is computed automatically. Next we set parameter *PT*.

6. Set a parameter of threshold *PT*. It is defined as: *PT*=(*minimum number of common frequency components*)/(*number of all differences in training set*). The minimum number of common frequency components is set experimentally. The parameter *PT* determines accuracy of expected results. We can analyze following example. Nine acoustic signals are generated H1, H2, H3, F1, F2, F3, R1, R2, R3, where H1, H2, H3 − test samples of the first class of acoustic signals, F1, F2, F3 − test samples of the second class of acoustic signals, R1, R2, R3 − test samples of the third class of acoustic signals. The frequencies in bold fonts are preselected by SMOFS-NFC. Let's suppose that SMOFS-NFC finds following frequency components: **100 Hz**, 200 Hz, 300 Hz for |H1-F1|, **99 Hz**, 220 Hz, **310 Hz, 620 Hz** for |H1-R1|, **99 Hz**, 110 Hz, 230 Hz, **309 Hz**, **310 Hz, 620 Hz** for |R1-F1|. **100 Hz**, 250 Hz, 350 Hz for |H2-F2|, **101 Hz**, 220 Hz, **311 Hz**, 340 Hz for |H2-R2|, 160 Hz, 260 Hz, **309 Hz** for |R2-F2|. **101 Hz**, 170 Hz, 270 Hz, **311 Hz** for |H3-F3|, **100 Hz**, 280 Hz, 380 Hz for |H3-R3|, 190 Hz, 290 Hz, **310 Hz, 620 Hz** for |R3-F3|. Frequency components 100 Hz and 310 Hz were found 3 times. We also find 99 Hz, 101 Hz, 311 Hz, 309 Hz. As we see there are no proper frequency component. 100 Hz is proper for |H-F| and |H-R|. However it is not proper for |R-F|. 310 Hz and 620 Hz are good for |R-F| and |H-R|. If we set *PT*=3/9=0.3333, then frequency components **100 Hz**, **310 Hz** and **620 Hz** are selected. It forms a group of frequency components. If we set *PT*=4/9=0.4444, then SMOFS-NFC finds 0 frequency components.
7. Find adjacent frequency components (100-1; 100+1; 310-1; 310+1) (100; 310). The range of adjacent frequency components should be selected experimentally. Let's consider the range of the 2 nearest frequency components: 99 Hz, 101 Hz, 309 Hz, 311 Hz. We need to set *PT*=2/9=0.2222. The SMOFS-NFC method finds frequency components: **99 Hz**, **100 Hz**, **101 Hz**, **309 Hz**, **310 Hz, 311 Hz.** However frequency component 620 Hz is not adjacent. If we use 4 nearest frequency components, SMOFS-NFC will find: (100-2; 100-1; 100+1; 100+2; 310-2; 310-1; 310+1; 310+2) (100; 310).
8. Use found adjacent frequency components to form feature vector.

The described SMOFS-NFC method is depicted in Fig. 9.

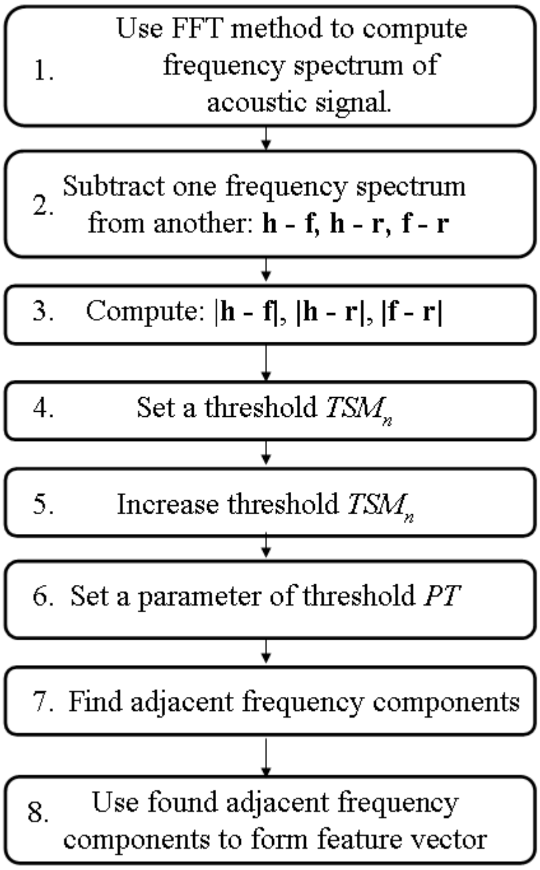

Figure 9. Steps of the SMOFS-NFC method

Rotating rotor, bearings, gears and other parts of the analyzed power tool generate acoustic signals. The authors analyzed 12 training samples of each type of acoustic signal (total 72 training samples). Following differences of spectra $|\mathbf{h} - \mathbf{f}|$, $|\mathbf{h} - \mathbf{r}|$, $|\mathbf{f} - \mathbf{r}|$ were computed and presented in figures 10–12. Feature extraction using SMOFS-NFC were presented (Fig. 10–12). For difference of spectra ($|\mathbf{h} - \mathbf{f}|$) SMOFS-NFC found 15 frequency coefficients (Fig. 10). For difference of spectra ($|\mathbf{h} - \mathbf{r}|$) SMOFS-NFC found 14 frequency coefficients (Fig. 11). For difference of spectra ($|\mathbf{f} - \mathbf{r}|$) SMOFS-NFC found 14 frequency coefficients (Fig. 12).

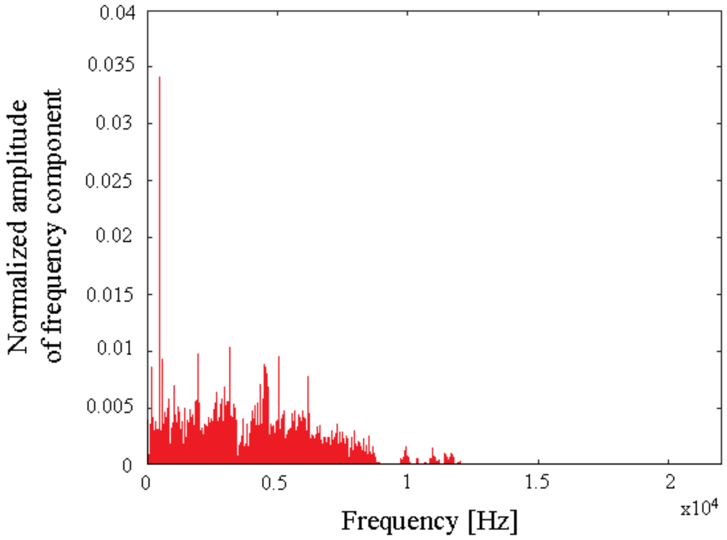

Figure 10. Difference of spectra (|**h** - **f**|) – step 3 of the SMOFS-NFC

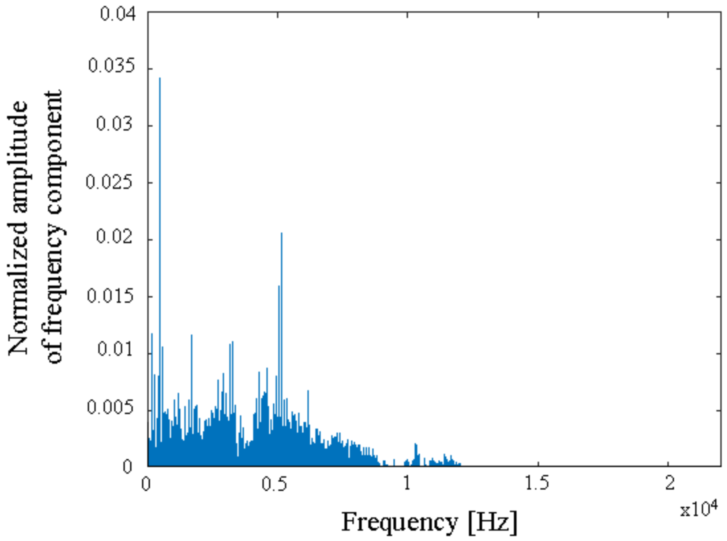

Figure 11. Difference of spectra (|**h** - **r**|) – step 3 of the SMOFS-NFC

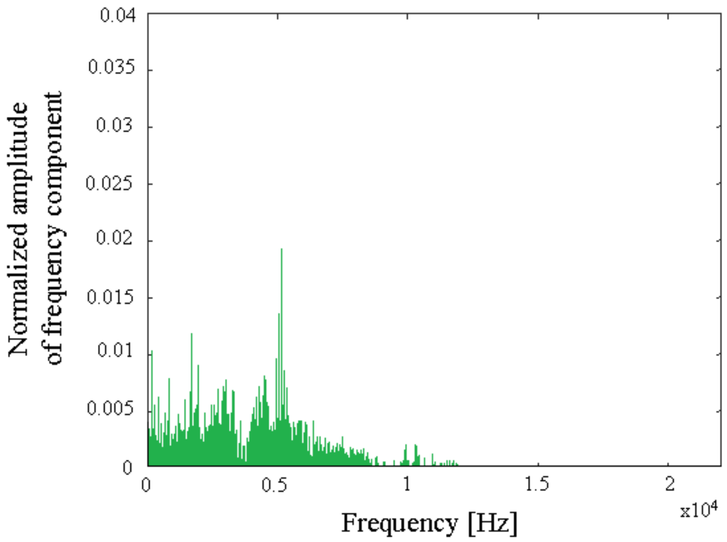

Figure 12. Difference of spectra (|**f** - **r**|) – step 3 of the SMOFS-NFC

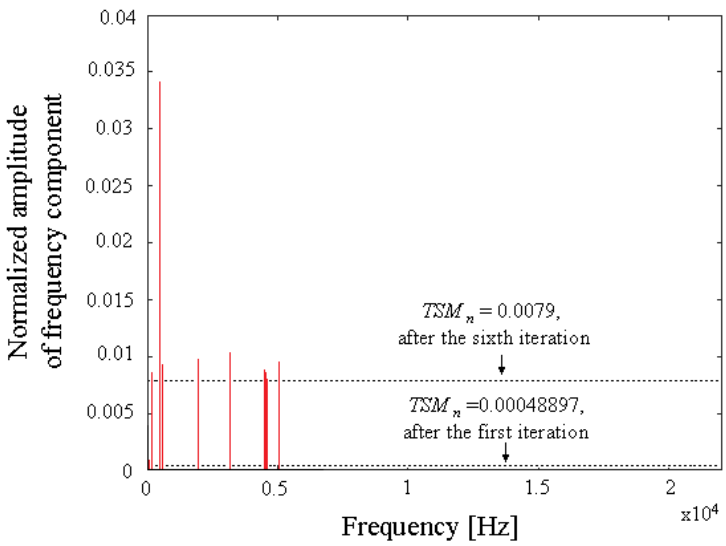

Figure 13. Feature extraction using SMOFS-NFC for difference (|**h - f**|) – step 5 of the SMOFS-NFC

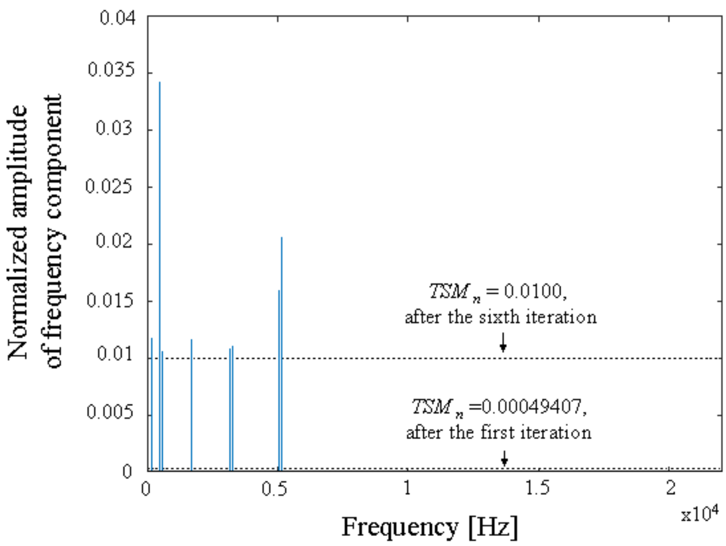

Figure 14. Feature extraction using SMOFS-NFC for difference (|**h - r**|) – step 5 of the SMOFS-NFC

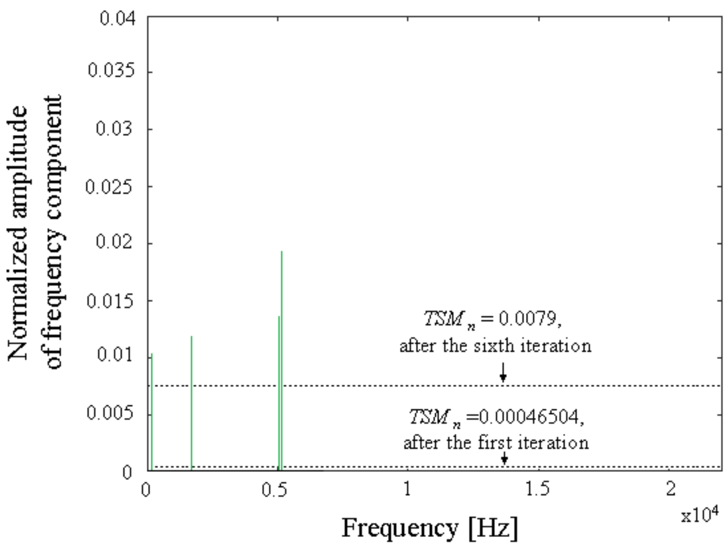

Figure 15. Feature extraction using SMOFS-NFC for difference (|**f - r**|) – step 5 of the SMOFS-NFC

Figures 10–15 show steps (2–5) of the SMOFS-NFC method. Next the method finds adjacent frequency components. Next the method uses found adjacent frequency components to form feature vector. It analyzes all training examples each other. The SMOFS-NFC method selected (for parameter *PT*=0.083=3/36) following adjacent frequency components of acoustic signal of the EID: 133, 149, 355, 356 Hz for SMOFS-0NFC, **132**, 133, **134**, **135**, **354**, 355, 356, **357** Hz for SMOFS-2NFC, **131**, 132, 133, 134, 135, **136**, **353**, 354, 355, 356, 357, **358** Hz for SMOFS-4NFC.

The SMOFS-NFC method selected (for parameter *PT*=0.083) following adjacent frequency components of acoustic signal of the AG: 428, 429, 430, 473, 474, 475, 476 Hz for SMOFS-0NFC, **427**, 428, 429, 430, **431**, **472**, 473, 474, 475, 476, **477** Hz for SMOFS-2NFC, **426**, 427, 428, 429, 430, 431, **432**, **471**, 472, 473, 474, 475, 476, 477, **478** Hz for SMOFS-4NFC.

Computed features (adjacent frequency components) of the EID are presented in figures 16–21.

Adjacent frequency components (8 features – SMOFS-2NFC) of acoustic signals of the healthy EID are presented (Fig. 16).

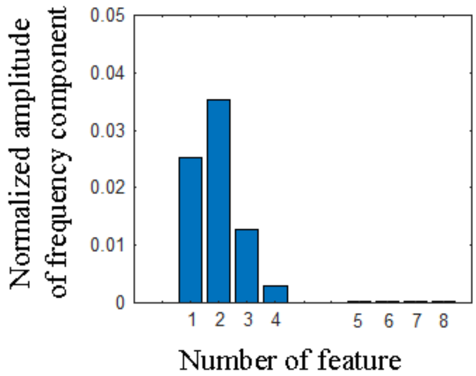

Figure 16. Feature vector of the healthy EID (8 features) – step 7 of the SMOFS-NFC

Adjacent frequency components (8 features – SMOFS-2NFC) of acoustic signals of the EID with damaged rear bearing are presented (Fig. 17).

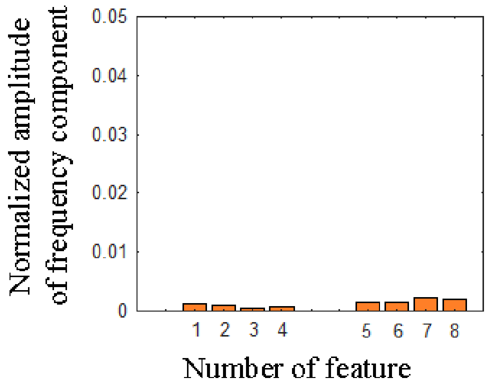

Figure 17. Feature vector of the EID with damaged rear bearing (8 features) – step 7 of the SMOFS-NFC

Adjacent frequency components (8 features – SMOFS-2NFC) of acoustic signals of the EID with damaged front bearing are presented (Fig. 18).

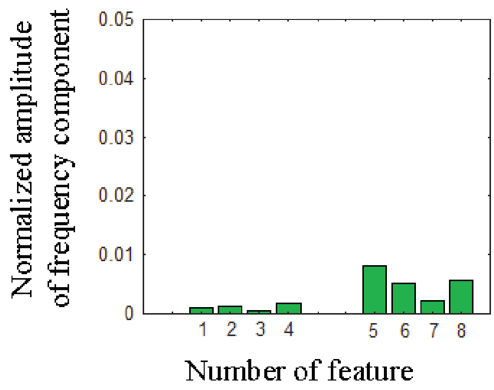

Figure 18. Feature vector of the EID with damaged front bearing (8 features) – step 7 of the SMOFS-NFC

Adjacent frequency components (12 features – SMOFS-4NFC) of acoustic signals of the healthy EID are presented (Fig. 19).

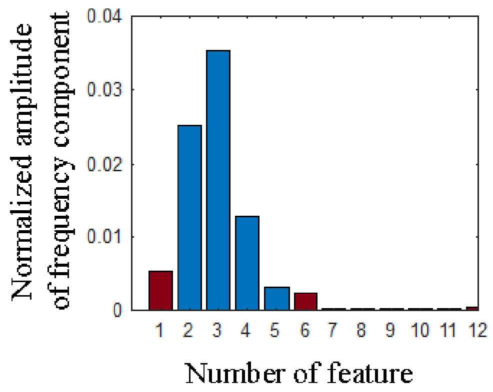

Figure 19. Feature vector of the healthy EID (12 features) – step 7 of the SMOFS-NFC

Adjacent frequency components (12 features – SMOFS-4NFC) of acoustic signals of the EID with damaged rear bearing are presented (Fig. 20).

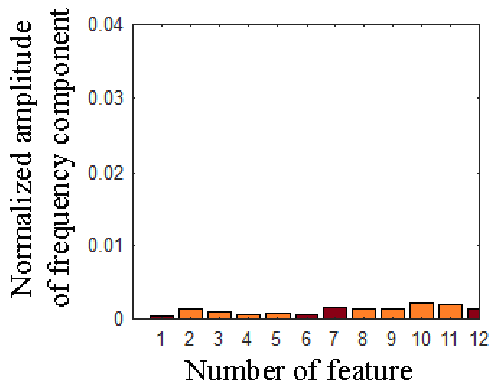

Figure 20. Feature vector of the EID with damaged rear bearing (12 features) – step 7 of the SMOFS-NFC

Adjacent frequency components (12 features – SMOFS-4NFC) of acoustic signals of the EID with damaged front bearing are presented (Fig. 21).

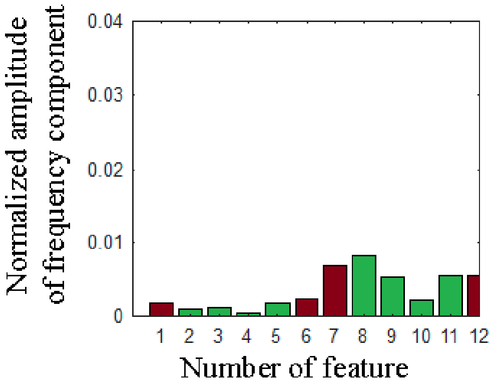

Figure 21. Feature vector of the EID with damaged front bearing (12 features) – step 7 of the SMOFS-NFC

Computed features (adjacent frequency components) of the angle grinder (AG) are presented in figures 22–27. Adjacent frequency components (11 features - SMOFS-2NFC) of acoustic signals of the healthy AG are presented (Fig. 22).

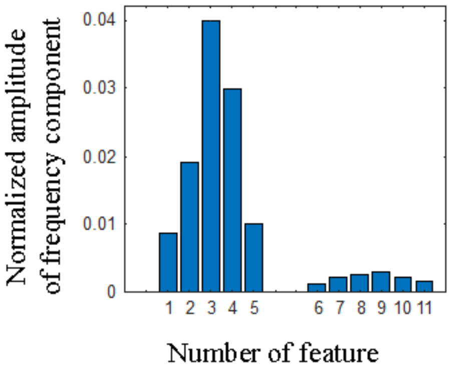

Figure 22. Feature vector of the healthy AG (11 features)

Adjacent frequency components (11 features - SMOFS-2NFC) of acoustic signals of the AG with 2 blocked air inlets are presented (Fig. 23).

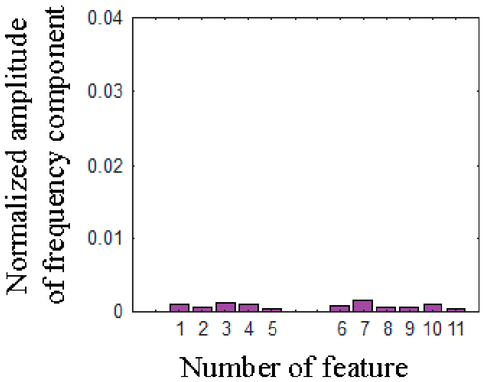

Figure 23. Feature vector of the AG with 2 blocked air inlets (11 features)

Adjacent frequency components (11 features - SMOFS-2NFC) of acoustic signals of the AG with 1 blocked air inlet are presented (Fig. 24).

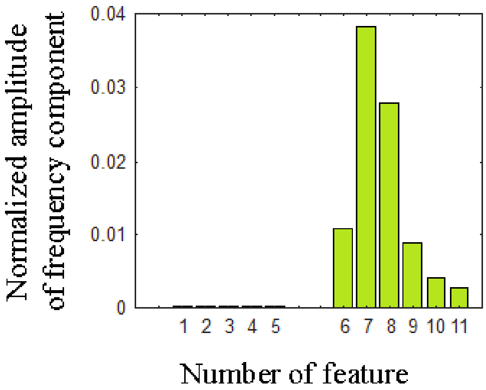

Figure 24. Feature vector of the AG with 1 blocked air inlet (11 features)

Adjacent frequency components (15 features - SMOFS-4NFC) of acoustic signals of the healthy AG are presented (Fig. 25).

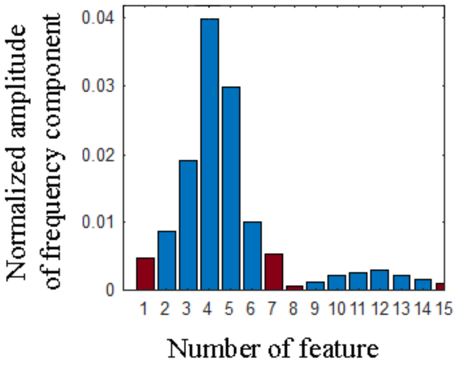

Figure 25. Feature vector of the healthy AG (15 features)

Adjacent frequency components (15 features − SMOFS-4NFC) of acoustic signals of the AG with 2 blocked air inlets are presented (Fig. 26).

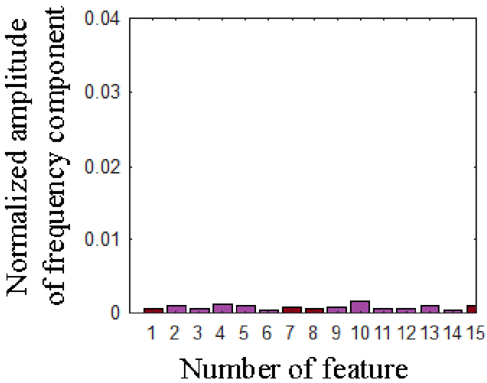

Figure 26. Feature vector of the AG with 2 blocked air inlets (15 features)

Adjacent frequency components (15 features - SMOFS-4NFC) of acoustic signals of the AG with 1 blocked air inlet are presented (Fig. 27).

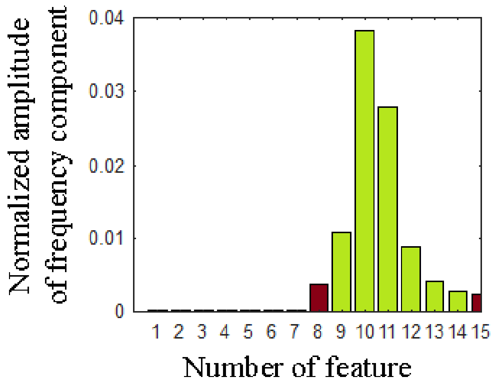

Figure 27. Feature vector of the AG with 1 blocked air inlet (15 features)

The authors used SMOFS-0NFC, SMOFS-2NFC, SMOFS-4NFC methods to extract features (figures 13–27). Acoustic features vectors were classified by the nearest neighbor classifier and Naive Bayes classifier. Other classification methods can be also considered.
Neural networks [37, 38, 39], Neuro-fuzzy systems [40], Support Vector Machine (SVM) [21, 41], fuzzy logic can be also proper for recognition. The authors used the Nearest Neighbor classifier and Naive Bayes classifier. They are fast and efficient. They can classify multidimensional vectors. The NN classifier allows us to check errors in the classification step.

4.2. The Nearest Neighbor classification method

The NN (Nearest Neighbor) is used for classification of data. It is a supervised machine learning method. It is used for many applications such as: text recognition, speaker recognition, sound recognition, image recognition, recognition of heart diseases, recognition of air quality, pattern recognition, fault diagnosis [42, 43, 44, 45]. The NN classifier finds distances between a new test vector and all training vectors. Next based on computed distance it selects the label of the closest training vector. This label is a result of classification.

Advantages of the NN classifier are: simplicity of implementation, we do not need to build a complex model, we do not need additional parameters and assumptions. It is versatile classifier. It can be used for many applications and problems. It has also some disadvantages. First we can have wrong nearest neighbor − noisy sample. If we use noisy sample, we will get wrong results. Next disadvantage is that the classifier gets slower if we have too many training samples. The authors used several similar training samples for each class. The acoustic signal was periodic, so the probability of noisy sample was decreased.

The Nearest Neighbor classifier can be used for different distance functions (metrics) − Manhattan, Euclidean, Minkowski distance etc. The authors used Manhattan distance. This distance metric is often used for the NN classifier. The Manhattan distance is defined as follows (4):

$$M(\mathbf{A},\mathbf{B}) = \sum_{i=1}^{p} |(a_i - b_i)| \tag{4}$$

where $M(\mathbf{A}, \mathbf{B})$ − is the Manhattan distance of vectors, $\mathbf{A}=[a_1,..., a_j]$ − is the test feature vector and $\mathbf{B}=[b_1,..., b_j]$ − is the training feature vector, p − number of frequency components (features), index $i=1,..., p$. The authors computed Manhattan distances for all features.

4.3.Naive Bayes classifier

Naive Bayes classifier is supervised machine learning method. It uses assumptions of naive independence between elements of the feature vectors. It is the probabilistic classification method. For test feature vector it computes a probability distribution of all analyzed classes. It finds application in text classification, real-time prediction, multi-class prediction, recommendation system, classification of incoming emails as spam or not spam, face recognition, fault diagnosis, classification of articles [46-48]. Naive Bayes classifier is defined as follows (5):

$$N_k = \underset{k \in \{1,\ldots,K\}}{\arg\max}\, P(N_k) \prod_{i=1}^{n} p(x_i \mid N_k) \tag{5}$$

where the prior probability of class N_k is denoted as $P(N_k)$; the likelihood of class N_k is denoted as $p(x_i | N_k)$; $1 \ldots n$ are elements of feature vectors; the assumption that $x_1, \ldots, x_n$ are conditionally independent; $1, \ldots, K$ are number of classes.

Advantages of Naive Bayes classifier are: small amount of training feature vectors are required for proper classification, easy to implement, it has high recognition rate for high-dimensional data points. More information about Naive Bayes classifier are available in following articles [46-48].

5. Results of acoustic fault diagnosis

Results of acoustic fault diagnosis were carried out for three same electric impact drills and three same angle grinders. Each power tool consisted of commutator motor and other parts such brushes, shaft, gear, gearwheels. Power tools were brand new. The authors made special faults that may occur during normal operation. Acoustic measurements were carried out in a room of 5 m x 4 m. Acoustic signals of healthy EID, EID with damaged rear bearing, EID with damaged front bearing, healthy angle grinder, angle grinder with 1 blocked air inlet, angle grinder with 2 blocked air inlets were measured and analyzed. Commutator motors of electric impact drills and angle grinders were powered by 230 V/50 Hz. Rated power of each motor was equal to 500 W. Weight of the EID was equal to 1.84 kg. Weight of the AG was equal to 1.64 kg. Rotor speed of the motor of the EID was equal to 3,000 rpm. Rotor speed of the motor of the AG was equal to 12,000 rpm. Considered motors operated without load.

The authors analyzed 100 test samples of healthy EID, 100 test samples of EID with damaged rear bearing, 100 test samples of EID with damaged front bearing. The authors analyzed 50 test samples of healthy AG, 50 test samples of AG with 1 blocked air inlet, 50 test samples of AG with 2 blocked. The authors analyzed 12 training samples of each type of acoustic signal (total 72 training samples).

The proposed approach used cross-validation for classification. Formula (6) was used for computation of performance results:

$$EF_{EID} = (S_{EID}) / (S_{ALL-EID}) \quad 100\% \tag{6}$$

where: S_{EID} – number of properly recognized test samples of test set (for example properly recognized test samples of healthy EID), $S_{ALL\text{-}EID}$ – number of all test samples of test set (all test samples of healthy EID), EF_{EID} – efficiency of recognition for one class of the EID (for example EF_{EID1} – healthy EID).

EF_{AG} – efficiency of recognition for one class of the AG (formula (7)) is computed similar to EF_{EID}.

$$EF_{AG} = (S_{AG}) / (S_{ALL-AG}) \quad 100\% \tag{7}$$

Formula (8) was used for computation of $EF_{EID\text{-}3\text{-}CLASSES}$ – efficiency of recognition for three classes of acoustic signal.

$$EF_{EID-3-CLASSES} = (EF_{EID1} + EF_{EID2} + EF_{EID3}) / 3 \tag{8}$$

where EF_{EID1} – EF_{EID} of the healthy EID, EF_{EID2} – EF_{EID} of the EID with damaged rear bearing, EF_{EID3} – EF_{EID} of the EID with damaged front bearing. $EF_{AG\text{-}3\text{-}CLASSES}$(formula (9)) is computed similar to $EF_{EID\text{-}3\text{-}CLASSES}$.

$$EF_{AG-3-CLASSES} = (EF_{AG1} + EF_{AG2} + EF_{AG3}) / 3 \tag{9}$$

Results of acoustic fault diagnosis of the EID using SMOFS-NFC (SMOFS-0NFC, SMOFS-2NFC, SMOFS-4NFC) and NN classifier were shown in Tables 1-3.

Table 1. Results of acoustic fault diagnosis of the EID using SMOFS-0NFC and NN classifier (4 features)

Type of acoustic signal	EF_{EID} [%]
Healthy EID	72
EID with damaged rear bearing	96
EID with damaged front bearing	100
	$EF_{EID\text{-}3\text{-}CLASSES}$ [%]
$EF_{EID\text{-}3\text{-}CLASSES}$ [%]	89.33

Table 2. Results of acoustic fault diagnosis of the EID using SMOFS-2NFC and NN classifier (8 features)

Type of acoustic signal	EF_{EID} [%]
Healthy EID	80
EID with damaged rear bearing	100
EID with damaged front bearing	100
	$EF_{EID\text{-}3\text{-}CLASSES}$ [%]
$EF_{EID\text{-}3\text{-}CLASSES}$ [%]	91.33

Table 3. Results of acoustic fault diagnosis of the EID using SMOFS-4NFC and NN classifier (12 features)

Type of acoustic signal	EF_{EID} [%]
Healthy EID	80
EID with damaged rear bearing	100
EID with damaged front bearing	100
	$EF_{EID\text{-}3\text{-}CLASSES}$ [%]
$EF_{EID\text{-}3\text{-}CLASSES}$ [%]	91.33

Results of acoustic fault diagnosis of the EID using SMOFS-NFC and Naive Bayes classifier were shown in Tables 4-6.

Table 4. Results of acoustic fault diagnosis of the EID using SMOFS-0NFC and Naive Bayes classifier (4 features)

Type of acoustic signal	EF_{EID} [%]
Healthy EID	96
EID with damaged rear bearing	92
EID with damaged front bearing	100
	$EF_{EID\text{-}3\text{-}CLASSES}$ [%]
$EF_{EID\text{-}3\text{-}CLASSES}$ [%]	96

Table 5. Results of acoustic fault diagnosis of the EID using SMOFS-2NFC and Naive Bayes classifier (8 features)

Type of acoustic signal	EF_{EID} [%]
Healthy EID	100
EID with damaged rear bearing	92
EID with damaged front bearing	100
	$EF_{EID\text{-}3\text{-}CLASSES}$ [%]
$EF_{EID\text{-}3\text{-}CLASSES}$ [%]	97.33

Table 6. Results of acoustic fault diagnosis of the EID using SMOFS-4NFC and Naive Bayes classifier (12 features)

Type of acoustic signal	EF_{EID} [%]
Healthy EID	100
EID with damaged rear bearing	92
EID with damaged front bearing	100
	$EF_{EID\text{-}3\text{-}CLASSES}$ [%]
$EF_{EID\text{-}3\text{-}CLASSES}$ [%]	97.33

Recognition efficiency for 3 classes $EF_{EID\text{-}3\text{-}CLASSES}$ was in the range of 89.33-91.33% for NN classifier. $EF_{EID\text{-}3\text{-}CLASSES}$ was in the range of 96-97.33% for Naive Bayes classifier.

The results of acoustic fault diagnosis of the AG using SMOFS-NFC and NN classifier were shown in Tables 7-9.

Table 7. Results of acoustic fault diagnosis of the AG using SMOFS-0NFC and NN classifier (7 features)

Type of acoustic signal	EF_{AG} [%]
Healthy AG	72
AG with 1 blocked air inlet	100
AG with 2 blocked air inlets	100
	$EF_{AG\text{-}3\text{-}CLASSES}$ [%]
$EF_{AG\text{-}3\text{-}CLASSES}$ [%]	90.66

Table 8. Results of acoustic fault diagnosis of the AG using SMOFS-2NFC and NN classifier (11 features)

Type of acoustic signal	EF_{AG} [%]
Healthy AG	80
AG with 1 blocked air inlet	100
AG with 2 blocked air inlets	100
	$EF_{AG\text{-}3\text{-}CLASSES}$ [%]
$EF_{AG\text{-}3\text{-}CLASSES}$ [%]	93.33

Table 9. Results of acoustic fault diagnosis of the AG using SMOFS-4NFC and NN classifier (15 features)

Type of acoustic signal	EF_{AG} [%]
Healthy AG	80

AG with 1 blocked air inlet	100
AG with 2 blocked air inlets	100
	$EF_{AG\text{-}3\text{-}CLASSES}$ [%]
$EF_{AG\text{-}3\text{-}CLASSES}$ [%]	93.33

The results of acoustic fault diagnosis of the AG using SMOFS-NFC and Naive Bayes classifier were shown in Tables 10-12.

Table 10. Results of acoustic fault diagnosis of the AG using SMOFS-0NFC and Naive Bayes classifier (7 features)

Type of acoustic signal	EF_{AG} [%]
Healthy AG	100
AG with 1 blocked air inlet	100
AG with 2 blocked air inlets	100
	$EF_{AG\text{-}3\text{-}CLASSES}$ [%]
$EF_{AG\text{-}3\text{-}CLASSES}$ [%]	100

Table 11. Results of acoustic fault diagnosis of the AG using SMOFS-2NFC and Naive Bayes classifier (11 features)

Type of acoustic signal	EF_{AG} [%]
Healthy AG	100
AG with 1 blocked air inlet	100
AG with 2 blocked air inlets	100
	$EF_{AG\text{-}3\text{-}CLASSES}$ [%]
$EF_{AG\text{-}3\text{-}CLASSES}$ [%]	100

Table 12. Results of acoustic fault diagnosis of the AG using SMOFS-4NFC and Naive Bayes classifier (15 features)

Type of acoustic signal	EF_{AG} [%]
Healthy AG	100
AG with 1 blocked air inlet	100
AG with 2 blocked air inlets	100
	$EF_{AG\text{-}3\text{-}CLASSES}$ [%]
$EF_{AG\text{-}3\text{-}CLASSES}$ [%]	100

Recognition efficiency for 3 classes $EF_{AG\text{-}3\text{-}CLASSES}$ was in the range of 90.66-93.33% for NN classifier. $EF_{AG\text{-}3\text{-}CLASSES}$ was equal to 100% for Naive Bayes classifier.

We can notice that SMOFS-0NFC computes same components frequency as SMOFS-MULTIEXPANDED method [23]. The proposed methods SMOFS-2NFC and SMOFS-4NFC compute more frequency components. SMOFS-2NFC and SMOFS-4NFC have higher recognition efficiency for 3 classes ($EF_{AG\text{-}3\text{-}CLASSES}$) than SMOFS-MULTIEXPANDED [23].

6. Discussion

Fault diagnosis is an essential task for many industrial processes. It ensures the safety of electrical and mechanical systems. Moreover, it enables to decide whether a fault has occurred or not. If faults have occurred, then they can be detected by diagnostic information such as: acoustic signals, vibration, temperature, electric current, voltage signals etc. Electrical faults can be detected by all mentioned signals. However, some of mechanical faults (for example faulty shaft) are difficult to detect using electrical or thermal signals. Acoustic signals are good for detection of both types of faults. However acoustic signals contain noise. The recognition results can be low if there are no training samples of specific fault in training set. The presented technique is based on training and test set. There is a need to capture similar acoustic signals from a similar motor. Appropriate microphone and appropriate distance from the microphone (tracer KTM 43948) to the motor are also required.

Several types of faults can be diagnosed by acoustic based technique. The authors analyzed bearings faults and ventilation faults. Other mechanical (faulty gears, faulty shafts, damaged sprockets) and electrical faults (broken rotor coils, shorted coils) can be also diagnosed similarly. The acoustic based approach is not expensive compared to thermal analysis or vibration analysis.

The SMOFS-NFC method has recognition results in the range of 89.33−100%. It is good method compared to other acoustic based fault diagnosis methods [20−30]. Adjacent frequency components are used in the analysis. Adjacent frequency components are slightly better than several frequency components (for example SMOFS-MULTIEXPANDED). The SMOFS-0NFC finds same frequency components as SMOFS-MULTIEXPANDED (Tab. 1, 4, 7, 10). SMOFS-2NFC and SMOFS-4NFC have higher recognition efficiency for 3 classes ($EF_{AG\text{-}3\text{-}CLASSES}$) than SMOFS-MULTIEXPANDED [23].

Analyzed Verto 50G515 electric impact drills (500 W) and Verto 51G053 angle grinders (500W) have similar construction as other power tools. The proposed approach based on the SMOFS-NFC method can be also used for different power tools and types of faults.

7. Conclusions and future work

Predictive maintenance of power tools is essential process in the industry. It prevents downtimes and accidents. It also decreases maintenance costs. Many fault diagnosis techniques have been developed to protect electrical motors. In this study, the authors analyzed following acoustic signals: healthy EID, EID with damaged rear bearing, EID with damaged front bearing, healthy AG, AG with 1 blocked air inlet, AG with 2 blocked air inlets.

The authors proposed the method of feature extraction SMOFS-NFC. The SMOFS-NFC (SMOFS-0NFC, SMOFS-2NFC, SMOFS-4NFC) was used to extract features of acoustic signals of power tools. Features were classified by the nearest neighbor classifier and Naive Bayes classifier. The authors analyzed 100 test samples of healthy EID, 100 test samples of EID with damaged rear bearing, 100 test samples of EID with damaged front bearing. The authors analyzed 50 test samples of healthy AG, 50 test samples of AG with 1 blocked air inlet, 50 test samples of AG with 2 blocked. The authors analyzed 12 training samples of each type of acoustic signal (total 72 training samples). The authors used supervised learning. Training and test sets were known for the authors. However computer knows only training set. Analysis showed that test set were analyzed properly by the computer. Moreover the proposed method was verified by thermal analysis.

The proposed analysis is efficient and has high recognition rate. The classification accuracy was in the range of 89.33-97.33% for three electric impact drills. The classification accuracy was in the range of 90.66-100% for three angle grinders.

The conducted analysis shows that:

1) The acoustic based fault diagnosis technique is proposed for detection of bearings faults and ventilation faults of power tools.
2) The acoustic based analysis is also useful for analysis of electrical and other mechanical faults of machines.
3) The SMOFS-NFC works well for analysis of acoustic signal of power tools.
4) The same microphone should be used to capture training and test set.

5) The same distance from the microphone to the motor should be used.

6) There is a need to use similar motors and machines for the analysis. It is difficult to recognize sound samples properly if we have different types of the motors for training and testing (for example motor of the train and motor of the electric drill).

The acoustic based analysis is useful for non-invasive fault diagnosis. This analysis is instant. The cost of equipment is about 350$. In the future the authors will develop the new acoustic based techniques. New feature extraction methods will be developed. It will be analyzed for noisy environment. In the future the authors will analyze microphone array and acoustic signals of electrical motors. Vibrations signals will be also analyzed. Different motors and types of faults will be also considered.

Funding: This work was supported in part by Generalitat Valenciana, Conselleria de Innovacion, Universidades, ´Ciencia y Sociedad Digital, (project AICO/019/224).

Conflicts of Interest: The author declares no conflict of interest.

References

1. El Hachemi Benbouzid M., A review of induction motors signature analysis as a medium for faults detection, *IEEE Transactions on Industrial Electronics* **2000**, 47(5), 984–993.
2. Liu MK., Tran MQ., Weng PY., Fusion of Vibration and Current Signatures for the Fault Diagnosis of Induction Machines, *Shock and Vibration* **2019**, Article Number: 7176482, DOI: 10.1155/2019/7176482.
3. Frini M., Soualhi A., El Badaoui M., Gear faults diagnosis based on the geometric indicators of electrical signals in three-phase induction motors, *Mechanism and Machine Theory* **2019**, 138, 1-15. DOI: 10.1016/j.mechmachtheory.2019.03.030
4. Candelo-Zuluaga C., Riba JR., Lopez-Torres C., Garcia A., Detection of Inter-Turn Faults in Multi-Phase Ferrite-PM Assisted Synchronous Reluctance Machines, Energies **2019**, 12(14), Article Number: 2733, DOI: 10.3390/en12142733.
5. Garcia-Bracamonte JE., Ramirez-Cortes JM., Rangel-Magdaleno JD., Gomez-Gil P., Peregrina-Barreto H., Alarcon-Aquino V., An Approach on MCSA-Based Fault Detection Using Independent Component Analysis and Neural Networks, *IEEE Transactions on Instrumentation and Measurement* **2019**, 68(5), 1353-1361, DOI: 10.1109/TIM.2019.2900143
6. Bessous N., Sbaa S., Megherbi AC., Mechanical fault detection in rotating electrical machines using MCSA-FFT and MCSA-DWT techniques, *Bulletin of the Polish Academy of Sciences-Technical Sciences* **2019**, 67(3), 571-582, DOI: 10.24425/bpasts.2019.129655
7. Kompella KCD., Mannam VGR., Rayapudi SR., Bearing fault detection in a 3 phase induction motor using stator current frequency spectral subtraction with various wavelet decomposition techniques, *Ain Shams Engineering Journal* **2018**, 9(4), 2427-2439. DOI: 10.1016/j.asej.2017.06.002
8. Gao YY., Yu DJ., Wang HJ., Fault diagnosis of rolling bearings using weighted horizontal visibility graph and graph Fourier transform, *Measurement* **2020**, Article Number: UNSP 107036, DOI: 10.1016/j.measurement.2019.107036
9. Wang L., Xiang JW., Liu Y., A time-frequency-based maximum correlated kurtosis deconvolution approach for detecting bearing faults under variable speed conditions, *Measurement Science and Technology* **2019**, 30(12), Article Number: 125005, DOI: 10.1088/1361-6501/ab3678
10. Zhu KH., Chen L., Hu X., A Multi-scale Fuzzy Measure Entropy and Infinite Feature Selection Based Approach for Rolling Bearing Fault Diagnosis, *Journal of Nondestructive Evaluation* **2019**, 38(4), Article Number: 90. DOI: 10.1007/s10921-019-0623-4

11. Tong SG., Huang YY., Jiang YQ., Weng YX., Tong ZM., Tang N., Cong FY., The identification of gearbox vibration using the meshing impacts based demodulation technique, *Journal of Sound and Vibration* **2019**, 461, Article Number: UNSP 114879, DOI: 10.1016/j.jsv.2019.114879.
12. Chen ZY., Gryllias K., Li WH., Mechanical fault diagnosis using Convolutional Neural Networks and Extreme Learning Machine, *Mechanical Systems and Signal Processing* **2019**, 133, DOI: 10.1016/j.ymssp.2019.106272
13. Kim S., Choi JH., Convolutional neural network for gear fault diagnosis based on signal segmentation approach, *Structural health monitoring-an international journal* **2019**, 18(5-6), 1401-1415. DOI: 10.1177/1475921718805683
14. Singh P., Harsha SP., Statistical and frequency analysis of vibrations signals of roller bearings using empirical mode decomposition, *Proceedings of the Institution of Mechanical Engineers Part K-Journal of Multi-body Dynamics* **2019**, 223(4), 856-870. DOI: 10.1177/1464419319847921
15. Li YB., Gu JX., Zhen D., Xu MQ., Ball A., An Evaluation of Gearbox Condition Monitoring Using Infrared Thermal Images Applied with Convolutional Neural Networks, *Sensors* **2019**, 19(9), Article Number: 2205, DOI: 10.3390/s19092205
16. Jeffali F., Ouariach A., El Kihel A., Nougaoui A., Infrared thermography based diagnosis of the impact on the kinematic chain, *Materials Today-Proceedings* **2019**, 13, 949-955, DOI: 10.1016/j.matpr.2019.04.059
17. Wahab AA., Abdullah NF., Rasid MAH., Commutator fault detection of brushed DC motor using thermal assessment, 1st International Postgraduate Conference on Mechanical Engineering (IPCME2018), *Book Series: IOP Conference Series-Materials Science and Engineering*, 2019, 469, DOI: 10.1088/1757-899X/469/1/012057
18. Jia Z., Liu ZB., Vong CM., Pecht M., A Rotating Machinery Fault Diagnosis Method Based on in Lure Learning of Thermal Images, *IEEE Access* **2019**, 7, 12348-12359. DOI: 10.1109/ACCESS.2019.2893331
19. Glowacz A., Fault diagnosis of electric impact drills using thermal imaging, Measurement, Volume 171, **2021**, DOI: 10.1016/j.measurement.2020.108815
20. Ramteke SM., Chelladurai H., Amarnath M., Diagnosis of Liner Scuffing Fault of a Diesel Engine via Vibration and Acoustic Emission Analysis, *Journal of vibration engineering & Technologies* **2019**, DOI: 10.1007/s42417-019-00180-7
21. Omoregbee HO., Heyns PS., Fault Classification of Low-Speed Bearings Based on Support Vector Machine for Regression and Genetic Algorithms Using Acoustic Emission, *Journal of vibration engineering & Technologies* **2019**, 7(5), 455-464. DOI: 10.1007/s42417-019-00143-y
22. Xiong W., He QB., Peng ZK., Separating Multiple Moving Sources by Microphone Array Signals for Wayside Acoustic Fault Diagnosis, *Journal of Vibration and Acoustics-Transactions of the ASME* **2019**, 141(5), DOI: 10.1115/1.4043508
23. Glowacz A., Fault diagnosis of single-phase induction motor based on acoustic signals, *Mechanical Systems and Signal Processing* **2019**, vol. 117, 65-80. DOI: 10.1016/j.ymssp.2018.07.044
24. Altaf M., Uzair M., Naeem M., Ahmad A., Badshah S., Shah JA., Anjum A., Automatic and Efficient Fault Detection in Rotating Machinery using Sound Signals, *Acoustics Australia* **2019**, 47(2), 125-139, DOI: 10.1007/s40857-019-00153-6
25. Sangeetha BP., Hemamalini S., Rational-Dilation Wavelet Transform Based Torque Estimation from Acoustic Signals for Fault Diagnosis in a Three-Phase Induction Motor, *IEEE Transactions on Industrial Informatics* **2019**, 15(6), 3492-3501, DOI: 10.1109/TII.2018.2874463
26. Parey A., Singh A., Gearbox fault diagnosis using acoustic signals, continuous wavelet transform and adaptive neuro-fuzzy inference system, *Applied Acoustics* **2019**, 147, 133-140. DOI: 10.1016/j.apacoust.2018.10.013
27. Hartono D., Halim D., Roberts GW., Gear fault diagnosis using the general linear chirplet transform with vibration and acoustic measurements, *Journal of Low Frequency Noise Vibration and Active Control* **2019**, 38 (1), 36-52. DOI: 10.1177/1461348418811717
28. Duan ZH., Wu TH., Guo SW., Shao T., Malekian R., Li ZX., Development and trend of condition monitoring and fault diagnosis of multi-sensors information fusion for rolling bearings: a review, *International Journal of Advanced Manufacturing Technology* **2018**, 96(1-4), 803-819, DOI: 10.1007/s00170-017-1474-8

29. Zhang DC., Stewart E., Entezami M., Roberts C., Yu DJ., Intelligent acoustic-based fault diagnosis of roller bearings using a deep graph convolutional network, Measurement, 2020, 156, DOI: 10.1016/j.measurement.2020.107585
30. Cichon A., Fracz P., Boczar T., Zmarzly D., Detection of Defects in On-Load Tap-Changers Using Acoustic Emission Method, *Conference Record of the 2012 IEEE International Symposium on Electrical Insulation (ISEI)*, **2012**, 184-188.
31. Machin G., Bojkovski J., del Campo D., Dogan, et al., A European roadmap for thermometry. *International Journal of Thermophysics* **2014**, *35*(3-4), 385-394.
32. Su J., Kochan O., Wang C., Kochan R., Theoretical and Experimental Research of Error of Method of Thermocouple with Controlled Profile of Temperature Field. *Measurement science review* **2015**, 15(6), 304-312.
33. Wang J., Kochan O., Przystupa K., Su J., Information-measuring System to Study the Thermocouple with Controlled Temperature Field. *Measurement Science Review* **2019**, 19(4), 161-169.
34. Kochan R., Kochan O., Chyrka M., Su J., Bykovyy P., Approaches of Voltage Divider Development for Metrology Verification of ADC, *In: Proceedings of the 2013 IEEE 7 International Conference on Intelligent Data Acquisition and Advanced Computing Systems IDAACS'2013* (pp. 70-76). Berlin, Germany.
35. Sun S, Przystupa K, Wei M, Yu H, Ye Z, Kochan O. Fast bearing fault diagnosis of rolling element using Levy Moth-Flame optimization algorithm and Naive Bayes. *Eksploatacja i Niezawodnosc – Maintenance and Reliability* **2020**; 22 (4): 730–740, http://dx.doi.org/10.17531/ein.2020.4.17
36. Jun S., Kochan O., Kochan R., Thermocouples with built-in self-testing. *International Journal of Thermophysics* **2016**, 37(4), 37.
37. Gajewski J., Valis D., The determination of combustion engine condition and reliability using oil analysis by MLP and RBF neural networks, *Tribology International* **2017**, 115, 557-572, DOI: 10.1016/j.triboint.2017.06.032
38. Z., Su, J., Jotsov, V., Kochan, O., Mykyichuk, M., Kochan, R & Sasiuk, T. Data Science Applications to Improve Accuracy of Thermocouples. In: *Proceedings 2016 IEEE 8th International Conference on Intelligent Systems* (pp. 180-188). Sofia, Bulgaria.
39. Zhang YG., Chen B., Pan GF., Zhao Y., A novel hybrid model based on VMD-WT and PCA-BP-RBF neural network for short-term wind speed forecasting, *Energy Conversion and Management* **2019**, 195, 180-197, DOI: 10.1016/j.enconman.2019.05.005
40. Caesarendra W., Wijayaa T., Tjahjowidodob T., Pappachana B.K., Weec A., Roslan M. I., Adaptive neuro-fuzzy inference system for deburring stage classification and prediction for indirect quality monitoring, *Applied Soft Computing* **2018**, 72, 565–578, DOI: 10.1016/j.asoc.2018.01.008.
41. Zhang Y., Hu HZ., Liu ZX., Zhao M., Cheng L., Concurrent fault diagnosis of modular multilevel converter with Kalman filter and optimized support vector machine, *Systems Science & Control Engineering* **2019**, 7(3), 43-53, DOI: 10.1080/21642583.2019.1650840
42. Hasan MJ., Kim JM., Fault Detection of a Spherical Tank Using a Genetic Algorithm-Based Hybrid Feature Pool and k-Nearest Neighbor Algorithm, *Energies* **2019**, 12(6), DOI: 10.3390/en12060991
43. Zhou Z., Li ZX., Cai ZD., Wang PL., Fault Identification Using Fast k-Nearest Neighbor Reconstruction, *Processes* **2019**, 7(6), DOI: 10.3390/pr7060340
44. Talavera-Llames R., Perez-Chacon R., Troncoso A., Martinez-Alvarez F., MV-kWNN: A novel multivariate and multi-output weighted nearest neighbours algorithm for big data time series forecasting, *Neurocomputing* **2019**, 353, 56-73. DOI: 10.1016/j.neucom.2018.07.092
45. Wang YX., Wang RJ., Li DF., Adu-Gyamfi D., Tian KB., Zhu YX., Improved Handwritten Digit Recognition using Quantum K-Nearest Neighbor Algorithm, *International Journal of Theoretical Physics* **2019**, 58(7), 2331-2340. DOI: 10.1007/s10773-019-04124-5
46. Trovato G., Chrupala G., Takanishi A., Application of the Naive Bayes Classifier for Representation and Use of Heterogeneous and Incomplete Knowledge in Social Robotics, *Robotics* **2016**, 5 (1), DOI: 10.3390/robotics5010006
47. Nam S., Hur J., Probabilistic Forecasting Model of Solar Power Outputs Based on the Naive Bayes Classifier and Kriging Models, *Energies* **2018**, 11(11), DOI: 10.3390/en11112982
48. Harzevili NS., Alizadeh SH., Mixture of latent multinomial naive Bayes classifier, *Applied Soft Computing* **2018**, 69, 516-527. DOI: 10.1016/j.asoc.2018.04.020